THE JOURNAL OF BIOLOGICAL CHEMISTRY VOL. 286, NO. 51, pp. 43902–43912, December 23, 2011
© 2011 by The American Society for Biochemistry and Molecular Biology, Inc. Printed in the U.S.A.

The WD40 Repeat Protein WDR26 Binds Gβγ and Promotes Gβγ-dependent Signal Transduction and Leukocyte Migration*[S]

Received for publication, September 6, 2011, and in revised form, November 3, 2011 Published, JBC Papers in Press, November 7, 2011, DOI 10.1074/jbc.M111.301382

Zhizeng Sun[‡1], **Xiaoyun Tang**[‡1], **Fang Lin**[§], **and Songhai Chen**[‡¶2]

From the Departments of [‡]*Pharmacology,* [§]*Anatomy and Cell Biology, and* [¶]*Internal Medicine, Roy J. and Lucille A. Carver College of Medicine, University of Iowa, Iowa City, Iowa 52242*

Background: How Gβγ regulates leukocyte migration through numerous signaling partners remains elusive.
Results: WDR26 binds Gβγ and is required for Gβγ signaling and leukocyte migration.
Conclusion: WDR26 is a novel Gβγ-binding partner that promotes Gβγ signaling and leukocyte migration.
Significance: Elucidating the signaling mechanisms of Gβγ is crucial for understanding its key role in many important cellular processes.

The Gβγ subunits of heterotrimeric G proteins transmit signals to control many cellular processes, including leukocyte migration. Gβγ signaling may regulate and be regulated by numerous signaling partners. Here, we reveal that WDR26, a member of the WD40 repeat protein family, directly bound free Gβγ *in vitro*, and formed a complex with endogenous Gβγ in Jurkat T cells stimulated by the chemokine SDF1α. Suppression of WDR26 by siRNAs selectively inhibited Gβγ-dependent phospholipase Cβ and PI3K activation, and attenuated chemotaxis in Jurkat T cells and differentiated HL60 cells *in vitro* and Jurkat T cell homing to lymphoid tissues in *scid* mice. Similarly, disruption of the WDR26/Gβγ interaction via expression of a WDR26 deletion mutant impaired Gβγ signaling and Jurkat T cell migration, indicating that the function of WDR26 depends on its binding to Gβγ. Additional data show that WDR26 also controlled RACK1, a negative regulator, in binding Gβγ and inhibiting leukocyte migration. Collectively, these experiments identify WDR26 as a novel Gβγ-binding protein that is required for the efficacy of Gβγ signaling and leukocyte migration.

G protein-coupled receptors (GPCRs)[3] comprise a large family of cell surface proteins that play an important role in many physiological functions, such as the sense of sight, smell, and taste, metabolism, neuronal activity, and cardiovascular homeostasis (1). GPCRs transmit extracellular signals through heterotrimeric G proteins, which are comprised of Gα and Gβγ subunits (1, 2). Both the Gα and Gβγ subunits can activate downstream effectors to relay signals from GPCRs.

Gβγ subunits play a prominent role in several cellular processes, including leukocyte migration (3–5). Leukocyte migration is directed by chemoattractants including bacterial by-products such as the formyl peptide, *N*-formyl-methionine-leucine-phenylalanine (fMLP), and a superfamily of chemotactic cytokines, chemokines, such as SDF1α and C5α. These chemoattractants act on GPCRs that primarily couple to pertussis toxin (PTX)-sensitive $G_{i/o}$ proteins. Previous work has shown that chemoattractants predominantly transmit chemotactic signals through Gβγ subunits liberated from the activated $G_{i/o}$ proteins (6–9). Free Gβγ activates diverse effectors including PI3Kγ (10–15), PLC$\beta_{2/3}$ (16), and guanine nucleotide exchange factors for Rac and Cdc42 (17–22) to direct leukocyte polarization and chemotaxis. However, although the critical role of Gβγ signaling and its downstream effectors in leukocyte migration has been well established, our understanding of how the activation of various Gβγ effectors is regulated spatially and temporally for precise control of directional cell migration remains limited (4, 23).

Gβ is a prototype of the WD40 repeat-containing protein family (24). These proteins are characterized by the presence of several repeats consisting of between 40 and 60 amino acids with two internal conserved dipeptide sequences, glycine-histidine (GH) and tryptophan-aspartic acid (WD) (24–27). These repeats form a circular bladed β-propeller structure, which defines multiple binding surfaces for diverse interacting proteins. Not surprisingly, many WD40 proteins primarily function as adaptor or scaffolding proteins to orchestrate the cellular localization and formation of signaling complexes (25).

Using Gβ1 as bait in a yeast two-hybrid screen, several WD40 repeat proteins were unexpectedly identified as binding partners of Gβγ (24, 28). The Gβ-interacting regions identified in this screen all reside in the WD40 region of these proteins, suggesting that the WD40 motif itself may mediate the interactions with Gβγ. We have previously characterized one of these interacting proteins, RACK1, and found that RACK1 binds to a

* This work was supported, in whole or in part, by National Institutes of Health Grant GM094255 (to S. C.) and American Heart Association Grant 10GRNT3620015 (to S. C.).
[S] The on-line version of this article (available at http://www.jbc.org) contains supplemental Figs. S1 and S2 and Videos S1 and S2.
[1] Both authors contributed equally to this paper.
[2] To whom correspondence should be addressed: Bowen Science Bldg., Rm. 2–3452, 51 Newton Rd., Iowa City, IA 52242. Tel.: 319-384-4562; Fax: 319-335-8930; E-mail: songhai-chen@uiowa.edu.
[3] The abbreviations used are: GPCR, G protein-coupled receptor; CUL4, cullin 4; DDB1, DNA damage-binding protein 1; dHL60, differentiated HL60; PTX, pertussis toxin; SCID, severe combined immunodeficiency; fMLP, *N*-formyl-methionine-leucine-phenylalanine; MBP, maltose-binding protein; PLC, phospholipase C; SDF1, stromal-derived cell factor-1.

side surface of Gβγ that overlaps with the binding sites of select Gβγ effectors, such as PI3Kγ and PLCβ$_2$ (29–31). Consequently, binding of RACK1 to Gβγ leads to selective inhibition of Gβγ signaling and impaired leukocyte migration (31). These findings indicate that RACK1 functions as a negative regulator that may confer signaling specificity of Gβγ.

WDR26 is another WD40-containing protein that was identified as a binding partner of Gβγ in the yeast two-hybrid screen (28). It is ubiquitously expressed and has been shown to protect neuronal cells from hydrogen peroxide-induced cell death (32, 33). Overexpression of the C-terminal fragment of WDR26 inhibited MEKK1-mediated transcription activities in COS7 cells (33), but promoted proliferation of a rat cardiomyoblast cell line (34). However, the molecular mechanisms underlying the activity of WDR26 are unknown. A recent proteomic analysis has identified WDR26 as one of many WD40 proteins associated with the cullin 4 (CUL4)-DNA damage-binding protein 1 (DDB1) ubiquitin E3 ligase complex, but whether WDR26 is involved in ubiquitin-mediated protein degradation has not yet been investigated (35).

In this study, we show that WDR26 binds free Gβγ both *in vitro* and in intact cells. Inhibition of WDR26 by siRNAs impaired Gβγ-mediated signal transduction and leukocyte migration *in vitro* and *in vivo*. By overexpressing a WDR26 fragment to perturb the Gβγ/WDR26 interaction, we further show that WDR26 mediates Gβγ signaling and leukocyte migration by acting on Gβγ. Taken together, our data establish for the first time that WDR26 functions as a novel binding partner of Gβγ that promotes Gβγ-dependent signal transduction and leukocyte migration.

EXPERIMENTAL PROCEDURES

Reagents—Human SDF-1α was from PreproTech. fMLP, PTX, and fibronectin were from Sigma. Fura-2/AM, Alexa 488-conjugated secondary antibodies and Alexa 568-conjugated phalloidin were from Invitrogen. Rabbit anti-AKT, mouse anti-phospho-AKT, rabbit anti-ERK1/2, and mouse anti-phospho-ERK1/2 antibodies were from Cell Signaling Technology, Inc. Rabbit anti-WDR26 was from Bethyl Laboratories. Rabbit anti-Gβ (T20) and mouse anti-RACK1 were from Santa Cruz Biotechnology.

Cell Culture—Jurkat T and HL60 cell lines (ATCC) were maintained in RPMI (Invitrogen) supplemented with 10% fetal bovine serum (FBS). HL60 cells (2×10^5/ml) were treated with 0.13% dimethyl sulfoxide to differentiate into human neutrophil-like cells (dHL60) (14, 31). HEK293 cells were grown in DMEM containing 10% FCS.

Transfection—Transient transfection of HEK293 cells was performed using Polyjet DNA *in vitro* transfection reagent (SignaGen). Transient transfection of Jurkat T and dHL 60 cells was achieved by using the Neon transfection system (Invitrogen) according to the manufacturer's protocol. For transfection of Jurkat T cells, 1×10^6 and 1×10^7 cells were used for 10 and 100 μl of electroporation tips, using the electroporation parameters, 1325 voltage/10 ms/4 pulse and 1350 voltage/10 ms/4 pulse, respectively. Transfection of dHL60 cells (1×10^6) was performed 5 days post-differentiation using 10 μl of electroporation tips and the electroporation parameters 1500 voltage/25 ms/1 pulse. Up to 80–90 and 90–100% transfection efficiency for plasmids and oligonucleotides, respectively, could be obtained as judged by the percentage of GFP- or fluorescence-positive cells 1-day post-transfection of plasmids encoding enhanced green fluorescent protein or FITC-labeled oligonucleotides. Cells were harvested for assays 48–62 h post-transfection.

Jurkat T cells stably expressing FLAG-WDR26 were generated after transduction with lentiviruses encoding the gene and selection with increasing concentrations of puromycin (0.2–10 μg/ml) for 4–6 weeks. Surviving cells were pooled and maintained in 1 μg/ml of puromysin.

siRNAs and DNA Constructs—Control siRNA targeting GFP or luciferase, siRNAs targeting human WDR26 gene sequences, siWDR26-1, 5′-ctaccaaattccgaaatcatt, and siWDR26-2, 5′-acaaagggatcggtgcctatt, were purchased from Dharmacon. A pool of four siRNAs targeting human cullin 4 was purchased from Santa Cruz Biotechnology. For transient transfection with the Neon transfection system, 100–250 pmol of siRNAs/10^6 cells were used.

The cDNAs for WDR26, and WDR26 deletion mutants WDR (1–122), WDR(123–231), WDR(232–661), and WDR(123–661) were generated by PCR. They were first cloned into the entry vector, pENTR/SD/D-TOPO, then destination vectors pcDNA3-DEST-FLAG, pcDNA3-DEST-mRFP, or pLenti CMV-DEST for expression in mammalian cells, pDEST8 for expression in Sf9 cells, or pMAL-DEST for expression in *Escherichia coli*, by using the Gateway cloning system (Invitrogen). The destination vectors pcDNA3-DEST-FLAG, pcDNA3-DEST-mRFP, and pMAL-DEST contain DNA sequences for epitope tags FLAG, mRFP, or maltose-binding protein (MBP) at the N-terminal of inserted genes.

Generation of Lentiviruses and Baculoviruses—Lentiviruses encoding FLAG-WDR26 were generated by transfecting HEK293FT cells with the pLenti-CMV-DEST vectors encoding FLAG-WDR26 together with the packaging vectors pMDL, pRSV, and pVSV using the Polyjet DNA *in vitro* transfection reagent (SignaGen) (36). The supernatant of culture media containing lentivirus was collected on days 2 and 3 post-transfection. Lentivirus was concentrated by ultracentrifugation (47,000 × *g* for 2 h) and resuspended in 0.2 ml of DMEM. Baculoviruses encoding FLAG-WDR26 were generated by using the Bac-To-Bac baculovirus expression system (Invitrogen) as described (30, 37).

Expression and Purification of Proteins—MBP, MBP-WDR26, and His-Gα$_i$-1 were expressed in *E. coli* BL21 cells and purified using amylose resin (New England Biolabs) and nickel-nitrilotriacetic acid-agarose (Qiagen), respectively (28, 30). Gβ1/His-γ2 was purified from Sf9 cells after infection with baculoviruses encoding the genes (37). FLAG-WDR26 was expressed by baculovirus infection of Sf9 cells and prepared as cell lysates in buffer (50 mM Tris-HCl, pH 8.0, 50 mM NaCl, 1 mM EDTA, 5 mM $MgCl_2$, 1 mM DTT, 0.2% Nonidet P-40), and stored as aliquots at −80 °C.

Interaction of WDR26 with Gα and Gβγ in Vitro—To determine its binding to Gα$_i$-1 or Gβ1γ2, FLAG-WDR26 was first immunoprecipitated from Sf9 cell lysates using the anti-FLAG M2 antibody (Sigma) followed by the protein G Dyna beads

(Invitrogen). The beads containing FLAG-WDR26 were then incubated with $G\alpha_i$-1 (0.2–5 μM) in the presence of 20 μM GDP, Gβ1γ2 (0.2–5 μM), or 0.5 μM $G\alpha_i$-1 plus 0.5 μM Gβ1γ2 in buffer (50 mM Tris-HCl, pH 8.0, 50 mM NaCl, 1 mM EDTA, 5 mM $MgCl_2$, 1 mM DTT, 0.2% Nonidet P-40) for 1 h at room temperature. Protein complexes were precipitated using a magnetic stand and subjected to SDS-PAGE and immunoblot analysis.

To measure the interaction of MBP or MBP-WDR26 with Gβ1γ2 using the spectrofluorometric assays, Gβ1γ2 was first labeled with 2-(4′-maleimidylanilino)naphthalene-6-sulfonic acid, sodium salt (M8, Invitrogen) as described (30, 38–40). Interaction of M8-labeled Gβ1γ2 with MBP-WDR26 or MBP was monitored at room temperature using a FluoroLog spectrofluorometer (HORIBA) with excitation at 322 nm and emission at 420 nm as reported (30).

Immunoprecipitation and Western Blotting Analysis—To co-immunoprecipitate FLAG-Gβ1γ2 with WDR26 and its mutants following their expression in HEK293 cells, cell lysates were prepared using modified RIPA buffer (50 mM Tris-HCl, pH 7.4, 150 mM NaCl, 1% Nonidet P-40, 1 mM EDTA) and protease inhibitors. FLAG-Gβ1γ2 was then immunoprecipitated using anti-FLAG M2 magnetic beads (Sigma). Protein complexes were resolved by SDS-PAGE and analyzed by Western blotting analysis.

To co-immunoprecipitate FLAG-WDR26 with endogenous Gβγ, Jurkat T cells were first serum-starved for 4–6 h and then stimulated with SDF1α for the indicated times. FLAG-WDR26 was immunoprecipitated from cell lysates and analyzed for forming a complex with Gβγ as described above.

Expression of various proteins was examined by Western blotting analysis using an Odyssey infrared imaging system (LI-COR Biosciences). To determine SDF1α (50 nM) and OKT3-mediated phosphorylation of ERK1/2 and AKT, Jurkat T cells were serum-starved for 4–6 h before stimulation.

Flow Cytometry—The expression level of CXCR4 in siRNA-treated Jurkat T cells was determined by labeling with the phycoerythrin-conjugated mouse anti-CXCR4 antibody (R & D Systems, Inc.), followed by flow cytometry analysis. Briefly, 48–62 h post-transfection, cells were washed with saline and then incubated with control IgG or phycoerythrin-conjugated mouse anti-human CXCR4 antibody (5 μg/ml) for 45 min at 4 °C. After washing with saline 3 times, cells were analyzed by flow cytometry (BD FACSCalibur).

Immunofluorescence Staining—To induce Jurkat T cell polarization, Jurkat T cells were suspended in serum-free RPMI containing 0.1% BSA and stimulated with control or SDF1α-conjugated sulfate latex beads for 5 min at 37 °C as described previously (31, 41). Polarization of dHL60 cells was performed by first placing cells onto fibronectin (100 μg/ml)-coated coverslips for 10 min at 37 °C. After unbound cells were washed away, the coverslips were assembled in a Zigmond chamber (42). An fMLP concentration gradient was established by filling one side of the chamber with Hanks' balanced salt solution (Invitrogen) containing 10 mM HEPES (pH 7.2) and 1% gelatin, and another side with the same buffer containing 100 nM fMLP. Cells were incubated at 37 °C for 15 min before fixation. Cells were fixed with 4% paraformaldehyde and permeabilized with 0.5% Triton X-100 for 5 min. Cells were stained with rabbit anti-WDR26 (1:1000) or anti-Gβ (1:400) at room temperature for 1 h, followed by incubation with the secondary antibody Alexa 488-conjugated anti-rabbit IgG and Alexa 568-conjugated phalloidin (1:200). Slides were visualized with a LSM510 Meta inverted confocal microscope (Carl Zeiss, Jena, Germany) with an argon/krypton laser and a Plan Apo 40 × 1.3 NA oil immersion lens (31). Images were acquired with LSM5 Image software (Carl Zeiss) and processed with Adobe Photoshop (San Jose, CA).

Cell Migration Assay—Transwell migration of Jurkat T cells was determined using a quantitative approach as described previously (29, 31). To measure chemotaxis of dHL60 cells in the Dunn chamber by time-lapse microscopy, cells were first seeded onto a coverslip pre-coated with 100 μg/ml of fibronectin for 10–20 min at 37 °C. The coverslip was then assembled with the Dunn chamber (43). The chemoattractant gradient was established by filling the inner well with modified Hanks' balanced salt solution (Invitrogen) containing 1% human serum albumin and the outer well with the same solution containing 100 nM fMLP. Images were taken every 30 s for 40 min at room temperature using an inverted microscope (Leica DMI6000B) equipped with a motorized stage. A Leica ×10, NA 0.3 Fluor DIC objective was used for imaging. Cell trajectories were tracked using Metamorph software (Molecular Devices, Sunnyvale, CA). To exclude undifferentiated cells or immobile cells resulting from deleterious effects of transient transfection, only cells moving in any directions for at least 10 μm in 30 min were included in the analysis. The migration speed was calculated as the total distance of cell movement divided by time, whereas the chemotaxis index was calculated as net distance of migration toward the direction of the fMLP source divided by the total distance moved (44). The directional change was calculated based on the average of each angle formed by the line drawn through the centroid of the cell parallel to the direction of the fMLP gradient and the line from the starting point of the cell to the next ending point for the whole period of cell migration (44).

Cell Homing in Vivo—Jurkat T cells treated with PTX or transiently transfected with a control or WDR26 siRNA were labeled with the fluorescence dye, carboxyfluorescein succinimidyl ester (Invitrogen). To normalize variations between different assays, untreated Jurkat T cells were labeled with 5-(and -6)-(((4-chloromethyl)benzoyl)amino)tetramethylrhodamine (Invitrogen), and mixed with an equal number of carboxyfluorescein succinimidyl ester-labeled cells (1×10^7) in 200 μl of saline and injected intravenously into the tail vein of a severe combined immunodeficiency (SCID) mouse (45, 46), based on an Institutional Animal Care and Use Committee-approved protocol at the University of Iowa. 3 h post-injection, cells were isolated from the bone marrow and spleen of the mouse and analyzed by flow cytometry (BD FACSCalibur) to identify the number of fluorescence-labeled cells that home to these tissues (45, 46). Data are expressed as the ratio of carboxyfluorescein succinimidyl ester-labeled cells to 5-(and -6)-(((4-chloromethyl)benzoyl)amino)tetramethylrhodamine-labeled untreated cells.

Measurement of Cytosolic Ca^{2+} Concentration—The cytosolic concentration of Ca^{2+} ($[Ca^{2+}]_i$) in Jurkat T and dHL60 cells was measured as previously described (36). Briefly, cells were

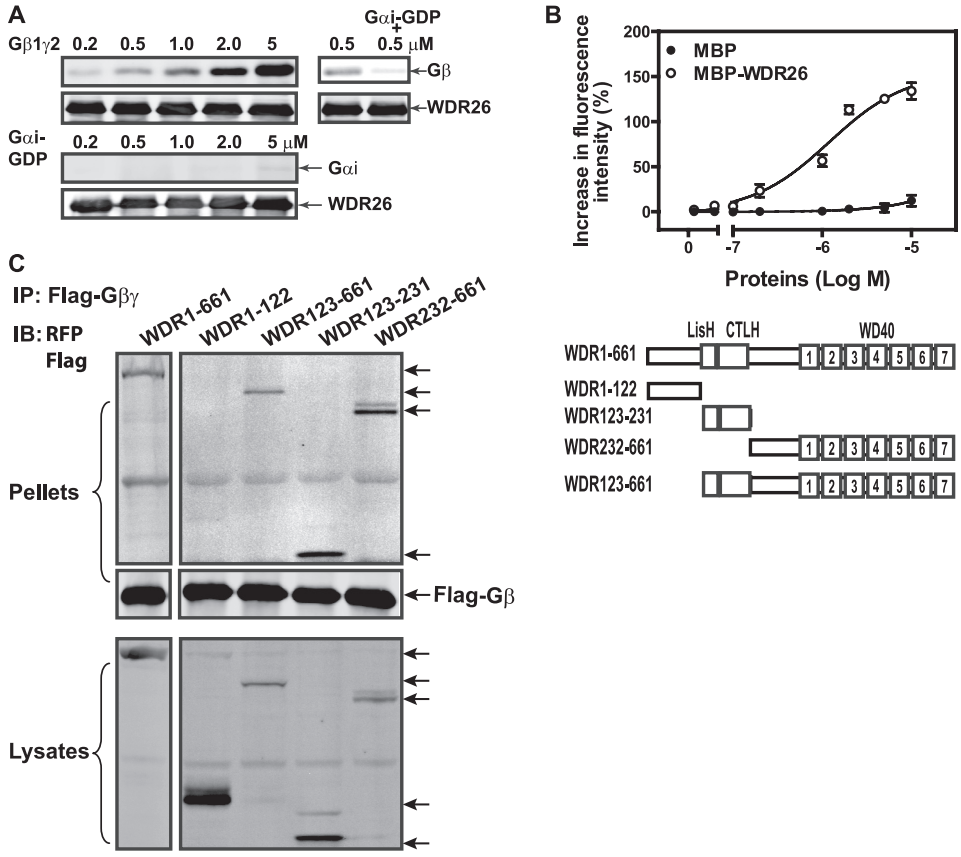

FIGURE 1. **Interaction of WDR26 with Gβγ.** *A,* direct binding of WDR26 to Gβγ *in vitro*. Binding of FLAG-WDR26 to increasing concentrations of purified Gβγ, $G\alpha_i$-1-GDP, or 0.5 μM Gβγ plus $G\alpha_i$-1-GDP was determined as described under "Experimental Procedures." Representative immunoblots from at least three separate experiments with similar results are shown. *B,* interaction of WDR26 with Gβγ characterized by fluorescence spectroscopy. Relative fluorescent changes of M8-labeled Gβ1γ2 as a function of purified MBP or MBP-WDR26 concentrations are shown. *C,* Gβγ interacts with WDR26 and its mutants in transfected HE293 cells. HEK293 cells were transfected with FLAG-Gβ1γ2 and RFP-tagged full-length WDR26 (WDR(1–661)) or the indicated WDR26 deletion mutants. Cell lysates were immunoprecipitated (*IP*) with an anti-FLAG antibody. The presence of proteins in the immunoprecipitates (pellets) and lysates was blotted (*IB*) for FLAG and RFP. *Arrows* indicate RFP-tagged WDR26 and its mutants. Schematic of the WDR26 structure and its mutants is shown in the *right panel*.

serum-starved for 4–6 h and loaded with 4 μM Fura 2/AM at room temperature for 40 min. The basal and agonist-stimulated changes in $[Ca^{2+}]_i$ were monitored at dual excitation wavelengths 340 and 380 nm and single emission wavelength 510 nm using a Biotek synergy 4 microplate reader (36). At the end of experiment, cells were first permeabilized with 2.5% Triton X-100 and then treated with 20 mM EGTA to obtain the fluorescent signal in the presence and absence of saturating amounts of Ca^{2+}. The cytosolic free Ca^{2+} concentration was calculated as described (47).

Measurement of Cyclic AMP—To measure SDF1α-mediated inhibition of cAMP production in Jurkat T cells, cells (1.5×10^6) were preincubated with 250 μM 3-isobutyl-1-methylxanthine for 20 min and then SDF1α (50 nM) for 10 min before stimulation with 10 μM forskolin for 20 min (29). cAMP levels were determined using the cAMP immunoassay system (Cell Biolabs, Inc.) according to the manufacturer's instructions.

Statistical Analysis—Data were expressed as mean ± S.E. Statistical comparisons between two groups were analyzed by two tailed Student's *t* test ($p < 0.05$ was considered significant).

RESULTS

WDR26 Binds Free Gβγ—To verify the result from the yeast two-hybrid screen showing that WDR26 binds Gβ1γ2, we performed *in vitro* binding assays using FLAG-tagged full-length WDR26 immunoprecipitated from Sf9 cells. As shown in Fig. 1*A*, WDR26 binds Gβ1γ2 in a dose-dependent manner, but did not bind GDP-bound $G\alpha_i$. Moreover, WDR26 binding to Gβ1γ2 was blocked by the presence of GDP-$G\alpha_i$, suggesting that WDR26 interacts with free Gβγ but not Gβγ in a heterotrimeric complex with Gα (Fig. 1*A*). To more accurately estimate the binding affinity, we used a fluorescence-based approach to monitor the binding of MBP-conjugated WDR26 to Gβ1γ2 labeled with an environmentally sensitive fluorescent probe, M8. As shown in Fig. 1*B*, the addition of MBP-WDR26 to M8-labeled Gβ1γ2 dose-dependently enhanced the intensity of fluorescence, presumably due to the increased hydrophobicity around the M8 fluorescent probe on Gβγ upon WDR26 binding. MBP alone had little effect. Based on this assay, the binding affinity for the WDR26/Gβ1γ2 interaction was estimated to be about 1 μM, which is comparable with that of Gβ1γ2 with other known binding partners including RACK1 (~0.5 μM) and $PLC\beta_2$ (~1 μM).

Database searches of conserved protein domains revealed that in addition to the WD40 repeats, WDR26 also contains a Lis-homology (LisH) and C-terminal to LisH (CTLH) domains at its N-terminal segment (Fig. 1*C*). To identify the binding sites

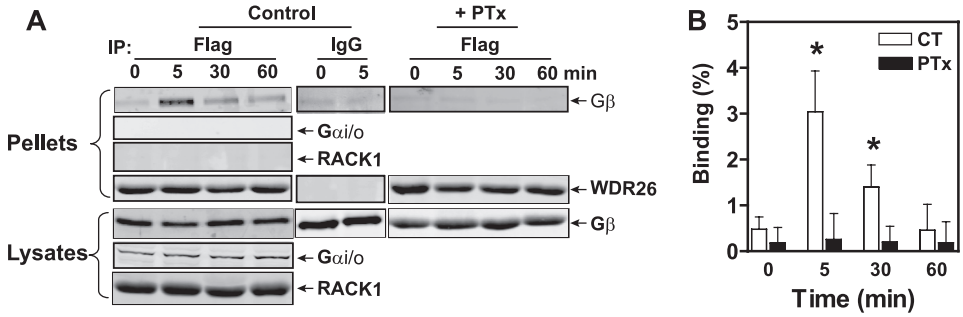

FIGURE 2. **WDR26 interacts with endogenous Gβγ.** FLAG-WDR26 was immunoprecipitated from Jurkat T cells pretreated with (*PTX*) or without (control; *CT*) pertussis toxin overnight and stimulated with SDF1α (50 nM) for the indicated time, using mouse IgG or an anti-FLAG antibody. The presence of Gβ, $G\alpha_{i/o}$, RACK1, and WDR26 in the immunoprecipitates (pellets) and lysates (2.5% of total) was detected with specific antibodies. Representative blots are shown in *A*, and quantitative data from three to four different experiments are shown in *B*. The amount of Gβγ binding to WDR26 is expressed as a percentage of total Gβγ in the lysates, with the background binding to mouse IgG subtracted. *, $p < 0.05$ indicates significance *versus* 0 min.

of Gβγ on WDR26, we constructed a series of deletion mutants of WDR26 conjugated with RFP and then expressed them together with FLAG-Gβ1γ2 in HEK293 cells (Fig. 1*C*). Co-immunoprecipitation assays indicate that the Gβγ-binding sites on WDR26 are located at the C terminus of WDR26 consisting of not only the WD40 domain but also the LisH-CTLH domain (Fig. 1*C*).

WDR26 Interacts with Endogenous Gβγ in Leukocytes—To test whether WDR26 interacts with endogenous Gβγ in cells, we stably expressed FLAG-tagged WDR26 in Jurkat T cells, because the commercially available antibodies for WDR26 and Gβ are not effective for immunoprecipitation. Co-immunoprecipitation analyses indicate that WDR26 had little association with Gβγ in unstimulated cells (Fig. 2, *A* and *B*). However, upon stimulation of Jurkat T cells with SDF1α, which activates the endogenous receptor CXCR4, WDR26 formed a complex with Gβγ within 5 min (Fig. 2, *A* and *B*). The association of WDR26 with Gβγ was decreased after prolonged stimulation, and was abolished by pre-treatment with PTX, indicating that $G_{i/o}$ proteins are involved. $G\alpha_{i/o}$ and RACK1 were not detected in the WDR26 precipitates from either stimulated or unstimulated cells (Fig. 2*A*), indicating that WDR26 selectively interacts with free Gβγ released from the activated heterotrimeric G proteins.

We then determined the cellular localization of WDR26 and Gβγ. Jurkat T cells treated with control beads were rounded and displayed little F-actin staining. In these cells, WDR26 was localized in the cytosol, whereas Gβγ was primarily distributed in the plasma membrane (Fig. 3, *A* and *B*). Stimulation with SDF1α-conjugated beads induced cell polarization and F-actin formation around the beads. In these cells, a substantial amount of Gβγ and WDR26 was found to be located at the plasma membrane where F-actin formed (Fig. 3, *A* and *B*), suggesting that SDF1α may induce WDR26 relocation and colocalization with Gβγ at the membrane. The translocation of WDR26 from the cytosol to the membrane was more evident in differentiated HL60 cells, a human neutrophil-like cell line that exhibits robust polarization in response to fMLP stimulation (supplemental Fig. S1). The polarized dHL60 cells displayed a well defined leading and trailing edge. In contrast to its uniform distribution in the cytosol of unstimulated cells, WDR26 was primarily detected at the leading edge of the polarized dHL60 cells where F-actin was located (supplemental Fig. S1). As we observed previously (31), Gβγ was distributed across the cell membrane of the polarized cells with a slightly increased accumulation at the leading edge (data not shown). These findings suggest that interaction with Gβγ is not solely responsible for membrane translocation of WDR26. However, pretreatment of dHL60 cells with PTX to block Gβγ activation inhibited both fMLP-stimulated dHL60 cell polarization and WDR26 translocation (supplemental Fig. S1), suggesting that Gβγ signaling may be required for WDR26 translocation.

WDR26 Is Required for Chemotaxis of Leukocytes—Chemoattractants such as SDF1α and fMLP transduce chemotactic signals for leukocyte migration primarily via Gβγ released from the activated $G_{i/o}$ proteins (3). Given that WDR26 specifically associates with Gβγ, we asked whether WDR26 plays a role in regulating Gβγ-mediated chemotaxis. We first evaluated the effect of WDR26 inhibition on Jurkat T cell migration. Transient transfection of siRNAs targeting two distinct regions of WDR26 led to specific inhibition of WDR26 expression, without affecting the expression of Gβγ or other proteins including the receptor CXCR4, $PLC\beta_2$, PI3Kγ, and RACK1 (Fig. 4, *A*–*C*). Down-regulation of WDR26 impaired the transwell migration of Jurkat T cells induced by SDF1α, but had no effect on the random migration of cells in the absence of SDF1α stimulation, suggesting that WDR26 specifically affects directional cell migration (Fig. 4*D*). In contrast, inhibition of CUL4, the ubiquitin ligase that binds WDR26 (35), did not affect cell migration (Fig. 4*D*), suggesting that the inhibitory effect of WDR26 suppression on chemotaxis is unlikely due to its impaired association with CUL4, and subsequent effects on ubiquitin-mediated protein degradation.

To determine whether WDR26 regulates leukocyte migration via its binding to Gβγ, we transiently expressed in Jurkat T cells an RFP-tagged C-terminal fragment of WDR26 (WDR(123–661)) (Fig. 4*E*), which contains the Gβγ-binding sites (Fig. 1*C*) and presumably competes with the full-length WDR26 for Gβγ binding. As a control, we also expressed RFP and an RFP-tagged N-terminal fragment of WDR26 (WDR(1–122)) (Fig. 4*E*) that did not bind Gβγ (Fig. 1*C*). Notably, as compared with cells expressing RFP, Jurkat T cells expressing WDR(123–661) but not WDR(1–122) exhibited a reduced response to SDF1α-stimulated chemotaxis (Fig. 4*F*), supporting the role of WDR26 interaction with Gβγ in mediating cell migration.

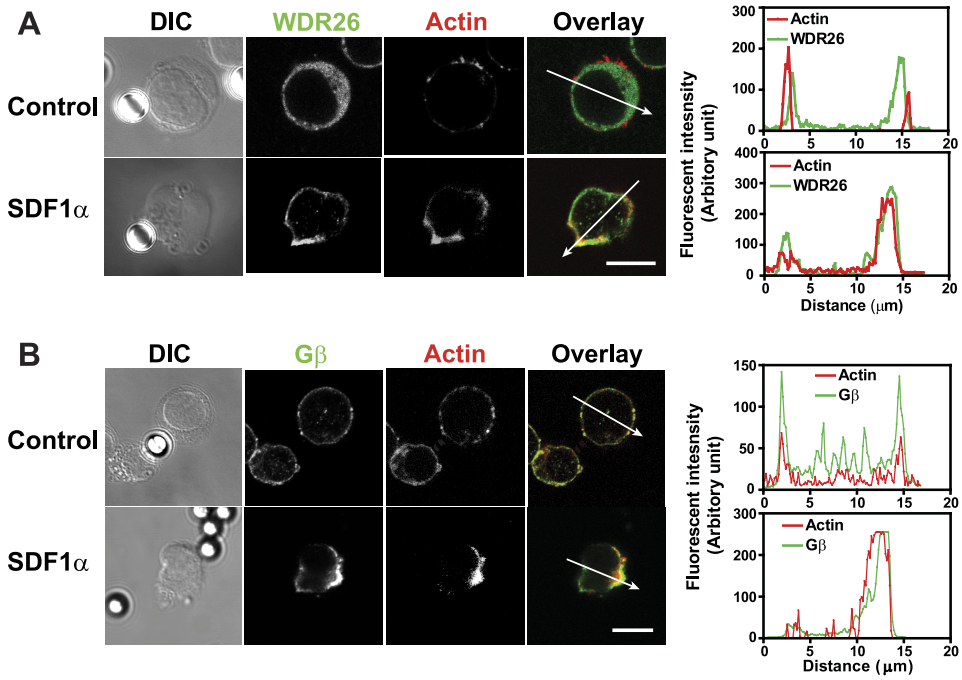

FIGURE 3. **Localization of WDR26 and Gβγ in Jurkat T cells.** Jurkat T cells were stimulated with control or SDF1α-coated sulfate latex beads. The cellular localization of WDR26 (*A*) and Gβγ (*B*) was revealed by first staining with rabbit anti-WDR26 and Gβ antibodies and then an Alexa 488-conjugated anti-rabbit IgG secondary antibody. F-actin was stained with Alexa 568-conjugated phalloidin. Distraction interference contrast (*DIC*) and fluorescent images are shown. *Bar*, 10 μm. The *right panel* shows the distribution of fluorescent intensity of WDR26, Gβ, and F-actin along the line drawn across the cells. The images are representatives of more than 30 cells from at least three separate experiments with similar results.

To further establish the functional significance of WDR26 in leukocyte trafficking *in vivo*, we adopted an *in vivo* homing assay in scid mice (45, 46). In this assay, Jurkat T cells were fluorescence-labeled and then injected into the mice by tail vein. The extent of cells homing to the lymphoid tissues, including spleen and bone marrow, was then evaluated 3 h post-injection. Previous work indicates that the homing of leukocytes to the lymphoid tissues relies on the activation of chemokine receptors expressed in leukocytes (45, 46). Consistent with this observation, pretreatment of cells with PTX to uncouple $G_{i/o}$ proteins from their cognate receptors led to impaired Jurkat T cell homing (Fig. 4*G*). Down-regulation of WDR26 had the similar inhibitory effect as PTX on the homing response (Fig. 4*G*). Together, these data indicate that WDR26 plays a critical role in chemotaxis of Jurkat T cell both *in vitro* and *in vivo*.

To determine whether WDR26 also plays a key role in the migratory response of other types of leukocytes, we extended our studies to dHL60 cells, which exhibit a robust chemotaxis response to fMLP stimulation, therefore enabling the migratory process to be monitored by the time-lapse microscopy. The chemotaxis of dHL60 cells was induced by a shallow and linear gradient of fMLP established in a Dunn chamber. As shown in Fig. 5, *A–C*, and supplemental Videos 1–2, although the control siRNA-treated cells preferentially migrated up the fMLP gradient in relatively straight paths, the WDR26-deficient cells moved in random directions with zigzag paths and took more turns in a short period. Supporting this, analysis of chemotaxis parameters indicates that as compared with the control cells, WDR26-deficient cells exhibited a decrease in migration speed and chemotaxis index (a measurement of how straight the cells move toward the higher concentration of the chemoattractant gradient), and an increase in the degrees of directional changes during the course of migration along the chemoattractant gradient (Fig. 5*D*). These findings indicate that inhibition of WDR26 impaired both the migratory ability and the directional sensing of dHL60 cells. Because fMLP-induced HL60 migration is also dependent on Gβγ-mediated signaling (48), these findings indicate that WDR26 plays a critical role in regulating Gβγ-dependent leukocyte migration.

WDR26 Controls Ability of RACK1 to Bind Gβγ and Inhibit Leukocyte Migration—We showed previously that RACK1 binds Gβγ and negatively regulates Gβγ-mediated leukocyte migration (31). Given that WDR26 and RACK1 are both expressed in leukocytes, and inhibition of WDR26 and RACK1 had opposite effects on leukocyte migration, it raises the possibility that WDR26 serves to counter-regulate the ability of RACK1 to bind Gβγ and inhibit Gβγ-mediated leukocyte migration. To test this, we determined the effect of WDR26 suppression on RACK1 binding to Gβγ. As we reported previously (31), co-immunoprecipitation studies show that the association of RACK1 to Gβγ was significantly increased after stimulation of Jurkat T cells with SDF1α for 30 min (Fig. 6, *A* and *B*). This is in contrast to WDR26, whose binding to Gβγ became evident within 5 min of SDF1α stimulation, and decreased after 30 min of SDF1α stimulation (Fig. 2, *A* and *B*). Moreover, significantly less Gβγ was co-immunoprecipitated with RACK1. This is probably due to the fact that the anti-RACK1 antibody immunoprecipitated only about 50% of total RACK1 from the lysates (data not shown), and/or a smaller fraction of RACK1 binding to Gβγ. Notably, inhibition of WDR26 abolished the association of RACK1 with Gβγ induced by SDF1α stimulation (Fig. 6, *A* and *B*), suggesting that WDR26 controls RACK1

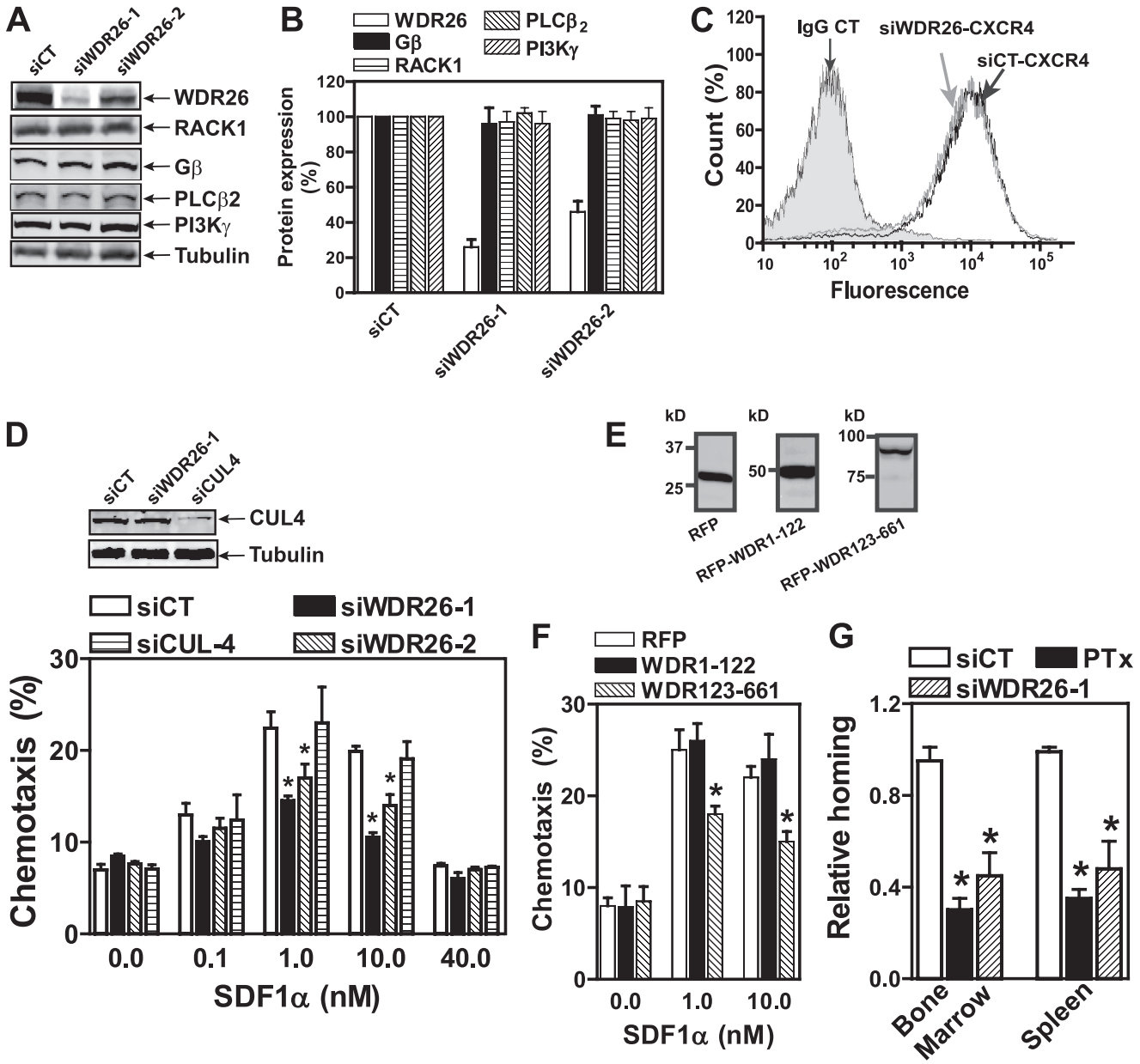

FIGURE 4. **WDR26 is required for leukocyte chemotaxis.** Jurkat T cells were transiently transfected with a control siRNA (siCT) or siRNAs targeting two distinct regions of WDR26 (siWDR26-1 and siWDR26-2), or CUL4 (siCUL-4). *A* and *B,* the expression level of the indicated proteins was determined by Western blotting analysis and quantified from three to six repeat experiments. *C,* CXCR4 expression was examined by staining the transfected cells with control IgG (*IgG CT*) or a phycoerythrin-conjugated anti-CXCR4 antibody, followed by flow cytometry analysis. *D,* chemotaxis was induced by the indicated concentrations of SDF1α and determined by the modified Boyden chamber assays. Chemotaxis was performed in triplicate and quantified from three to six repeat experiments. *Inset*, representative blots showing CUL-4 and tubulin expression in the transfected cells. *E* and *F,* the effect of overexpressing WDR26 mutants on chemotaxis of Jurkat T cells transiently transfected with RFP, RFP-WDR(1–122), or RFP-WDR(123–661) ($n = 3$). The expression level of the indicated proteins is shown in the blots (*E*). *G,* the effect of suppressing WDR26 on Jurkat T cell homing in *scid* mice. Jurkat T cells were treated with PTX (0.2 μg/ml overnight), or transfected with a control (*siCT*) or WDR26 siRNA (*siWDR26*), and then injected into the tail vein of the mice. 3 h post-injection, the homing of Jurkat T cells to the bone marrow and spleen was analyzed by flow cytometry. Data are calculated from three to four repeat experiments and expressed as the fraction of control cells homing to the indicated tissues. *, $p < 0.05$ indicate significant difference *versus* siCT or RFP.

interaction with Gβγ, rather than simply competes with RACK1 for Gβγ binding. To determine whether WDR26 functions upstream of RACK1 to regulate its ability to inhibit Gβγ-mediated leukocyte migration, we evaluated the effect of suppressing WDR26 and RACK1 either alone or simultaneously on Jurkat T cell migration. Although silencing either RACK1 or WDR26 alone led to a similar degree of change in Jurkat T cell migration, simultaneous suppression of RACK1 and WDR26 did not restore normal cell migration. Cells with deficiency in both WDR26 and RACK1 exhibited a similar degree of decrease in migration as the WDR26-deficient cells (Fig. 6*C*), indicating that WDR26 is essential for leukocyte migration. Collectively, these data suggest that WDR26 likely functions upstream of RACK1 in regulating Gβγ-mediated leukocyte migration.

WDR26 Promotes Gβγ-dependent Signal Transduction—Gβγ activates a diverse set of downstream effectors, including PLCβ and PI3K to regulate leukocyte migration (3). To determine whether WDR26 contributes to leukocyte migration by

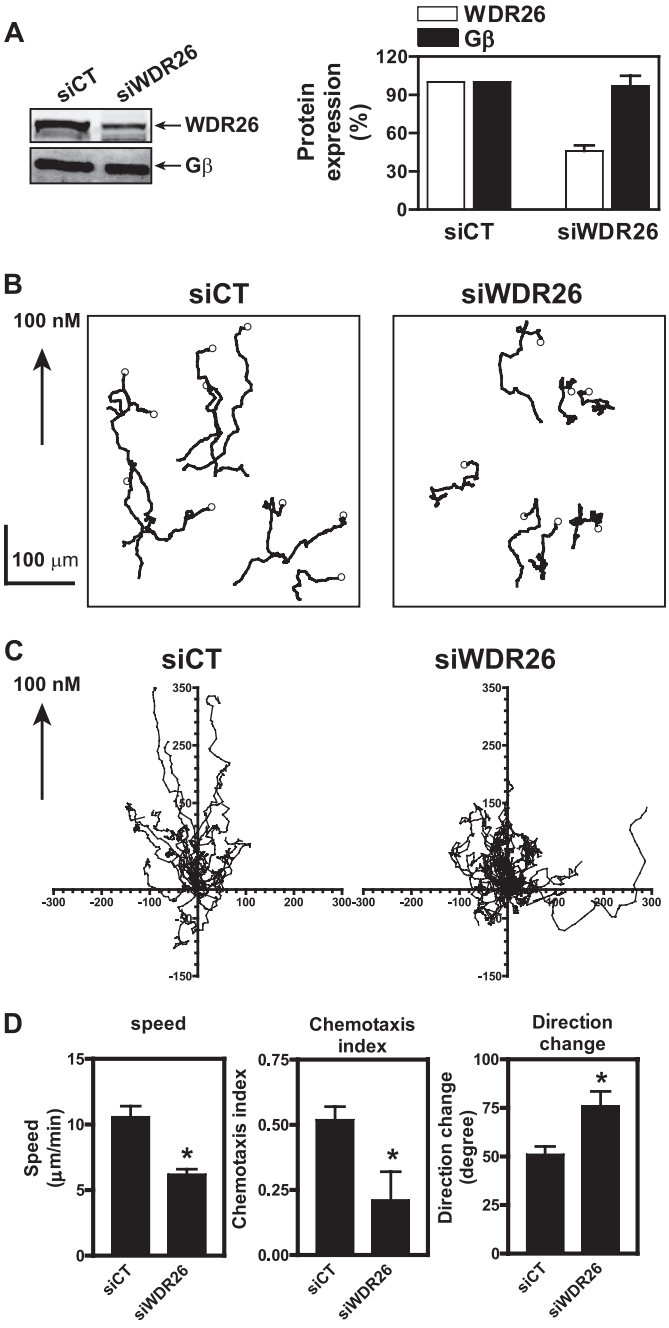

FIGURE 5. **WDR26 regulates chemotaxis of dHL60 cells.** dHL60 cells were transiently transfected with a control (siCT) or WDR26 siRNA. *A,* WDR26 and Gβ expression in the transfected cells is shown by representative immunoblots and quantitative data ($n = 3$). *B,* chemotaxis of the transfected cells was monitored by time-lapse imaging analysis for 30 min at room temperature in a stable gradient of fMLP (0–100 nM) established in a Dunn chamber. Migration paths of the transfected cell from one representative experiment are shown. *Open cycles* mark the end position of migrating cells. *C,* trajectories of siCT and siWDR26-transfected cells ($n > 23$ cells) from at least three separate experiments. The starting point for each cell is plotted to the origin of *x* and *y* axes. *Arrows* indicate the direction of the fMLP concentration gradient from 0 to 100 nM. *C,* the parameters of chemotaxis calculated from the experiment in *B*. *, $p < 0.05$ indicate significance *versus* siCT.

modulating Gβγ signaling, we evaluated the effect of WDR26 inhibition on SDF1α-stimulated Ca^{2+} signaling, and AKT and ERK1/2 phosphorylation in Jurkat T cells, which are known to be mediated by Gβγ (8, 10, 31). Suppressing WDR26 significantly reduced SDF1α-stimulated Ca^{2+} signaling and AKT phosphorylation, but had little effects on ERK1/2 phosphorylation (Fig. 7, *A–D*), although the activation of these signaling pathways was equally sensitive to PTX-mediated inhibition (data not shown), suggesting the involvement of Gβγ. Similar results were found in dHL60 cells transfected with WDR26 siRNAs (supplemental Fig. S2). The effect of WDR26 inhibition is specific to Gβγ signaling, because it affected neither $G\alpha_i$-mediated inhibition of cAMP accumulation nor the increase in Ca^{2+} signaling stimulated by OKT3 through the T-cell receptor (Fig. 7, *A* and *E*). Together, these findings indicate that WDR26 promotes the activation of selective signaling pathways mediated by Gβγ in leukocytes.

To seek further evidence that WDR26 regulates Gβγ signaling by acting on Gβγ, we measured SDF1α-stimulated AKT phosphorylation in Jurkat T cells expressing RFP, RFP-WDR(1–122), or RFP-WDR(123–661). As compared with RFP, overexpression of RFP-WDR(1–122) had no effect on AKT phosphorylation (Fig. 7*F*). In contrast, overexpression of WDR(123–661) led to a significant decrease in AKT phosphorylation (Fig. 7*F*). Because WDR(123–661) but not WDR(1–122) binds Gβγ, these data suggest that WDR26 regulates Gβγ signaling via interaction with Gβγ.

DISCUSSION

In this study, we have demonstrated that WDR26 serves as a novel binding protein of Gβγ that promotes Gβγ-dependent signal transduction and leukocyte migration. Data from both *in vitro* and *in vivo* binding assays support the specific binding of WDR26 to free Gβγ but not Gβγ in the heterotrimers or to Gα subunits. Such interaction likely involves subcellular relocation of WDR26 because in quiescent cells, WDR26 primarily localizes to the cytosol, whereas Gβγ is located in the plasma membrane. As demonstrated by confocal microscopic and co-immunoprecipitation studies, activation of Gβγ leads to WDR26 translocation from the cytosol to the plasma membrane and also an enhanced interaction between Gβγ and WDR26. Interestingly, in the polarized human neutrophil-like dHL60 cells, WDR26 accumulates primarily at the leading edge of cells, whereas Gβγ is distributed only in a shallow gradient from the leading edge to the trailing edge (31). These findings suggest that the recruitment of WDR26 to the leading edge of the polarized cells is unlikely to be simply anchored through Gβγ. Rather, it may also involve Gβγ-dependent signaling because blocking Gβγ activation with PTX inhibits WDR26 translocation.

The functional importance of WDR26 interaction with Gβγ is demonstrated by the findings that suppressing WDR26 impaired SDF1α-induced Jurkat T cell migration *in vitro* and also the homing of these cells to lymphoid tissues *in vivo*. Moreover, the chemotactic response of dHL60 cells to a shallow gradient of fMLP was significantly suppressed by WDR26 inhibition. SDF1α and fMLP transmit chemotactic signals through distinct GPCRs, CXCR4 and formyl peptide receptors, but both receptors primarily couple to PTX-sensitive $G_{i/o}$ proteins and signal via Gβγ. Given that WDR26 interacts with Gβγ, these findings suggest that WDR26 likely regulates leukocyte migration by acting on Gβγ rather than on receptors.

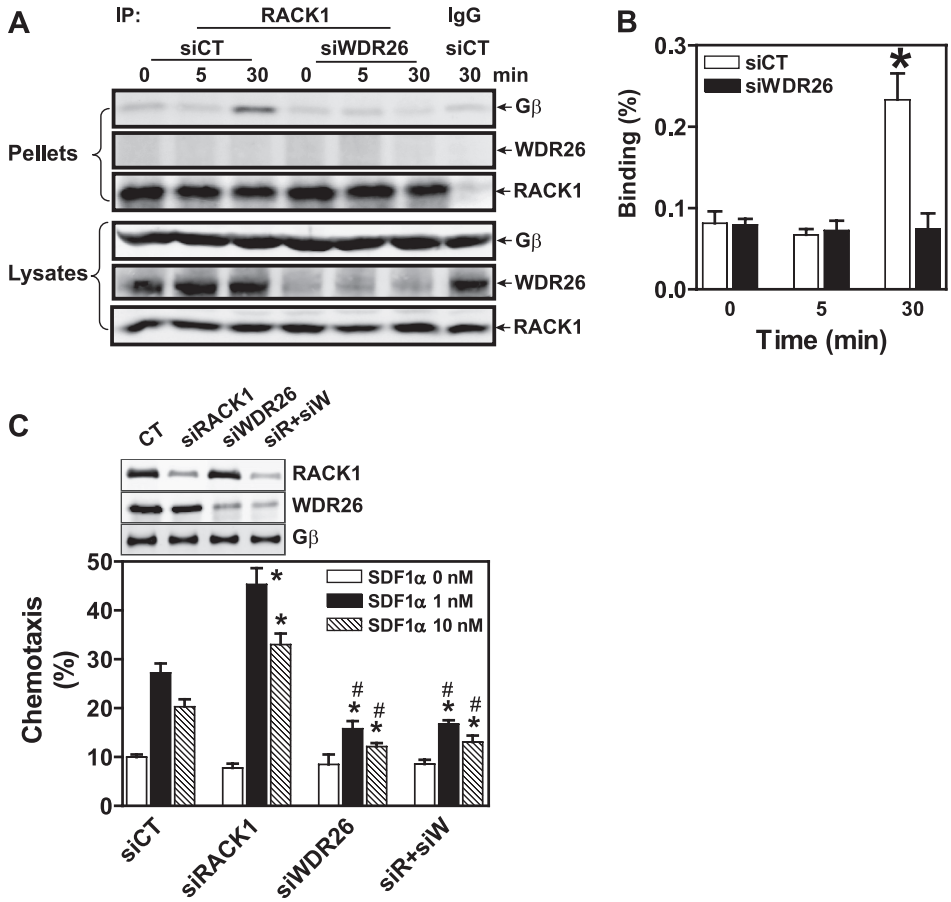

FIGURE 6. **WDR26 controls the ability of RACK1 to bind Gβγ and inhibit chemotaxis.** *A* and *B*, Jurkat T cells transiently transfected with a control (*siCT*) or WDR26 siRNA (*siWDR26*) were stimulated with SDF1α (50 nM) for the indicated time. Cell lysates were immunoprecipitated (*IP*) with mouse IgG control or a mouse anti-RACK1 antibody. The presence of Gβγ, WDR26, and RACK1 in the precipitates (*pellets*) and lysates (2.5% of total) was detected with specific antibodies. Representative blots are shown in *A*, and quantitative data from three to four different experiments are shown in *B*. The amount of Gβγ binding to RACK1 is expressed as a percentage of total Gβγ in the lysates, with the background binding to mouse IgG substracted. *C*, chemotaxis was determined in Jurkat T cells transiently transfected with a control siRNA (*siCT*), or siRNAs against WDR26 (*siWDR26*) or RACK1 (*siRACK1*) either individually or in combination (*siR*+*siW*) ($n = 3$). Chemotaxis was induced by SDF1α (0, 1, and 10 nM) for 3 h. * and #, $p < 0.05$ indicate significance *versus* siCT and siRACK1, respectively.

Gβγ transmits chemotactic signals for leukocyte migration through several downstream effectors, including PI3Kγ and PLC$\beta_{2/3}$ (3, 49). Our data indicate that WDR26 regulates leukocyte migration by selectively promoting Gβγ-dependent signal transduction. This is evident from the data showing that down-regulation of WDR26 alleviated SDF1α- or fMLP-stimulated Ca^{2+} signaling and AKT phosphorylation in Jurkat T cells or dHL60 cells. Moreover, suppressing WDR26 affects neither TCR-stimulated Ca^{2+} signaling nor a $G\alpha_{i/o}$-mediated decrease in cAMP production or ERK1/2 activation, indicating that WDR26 is required for the activation of specific Gβγ effectors. The ability of WDR26 to regulate Gβγ signaling and leukocyte migration likely depends on its binding to Gβγ, because Jurkat T cell migration is inhibited by the WDR26 deletion mutant (WDR(123–661)) that binds Gβγ, but not by the mutant (WDR(1–122)) that fails to bind Gβγ. In addition to PI3K and PLCβ, it has been shown that Gβγ may activate other signaling pathways including those mediated by PLA_2 and p38 MAPKs to regulate leukocyte migration (50–54). It remains to be determined whether WDR26 is also required for the activation of these pathways by Gβγ. Moreover, it will be interesting to determine whether WDR26 also links Gβγ to other unknown pathways that control leukocyte migration. In this sense, WDR26 may function as an effector rather than simply a regulator of Gβγ.

It is well established that PI3Kγ and PLC$\beta_{2/3}$ can be activated by Gβγ via protein-protein interactions *in vitro* (4), but how they are activated by Gβγ in cells and how the activation is regulated remain to be resolved. We showed previously that Gβγ-mediated PI3Kγ and PLCβ activation is negatively regulated by RACK1, which competes with PI3Kγ and PLCβ for binding Gβγ (31). Given that the function of WDR26 in regulating Gβγ is opposite to that of RACK1, WDR26 may simply counter-regulate the activity of RACK1 in Gβγ signaling. However, we found that suppressing WDR26 did not increase RACK1 binding to Gβγ, but, rather, abolished RACK1 binding to Gβγ. Moreover, down-regulation of RACK1 could not rescue the migratory defect of Jurkat T cells with deficiency in WDR26, indicating that WDR26 functions upstream of RACK1. These findings suggest a possible scenario that, in response to chemoattractants, WDR26 and RACK1 may alternately interact with Gβγ to fine-tune Gβγ signaling for leukocyte migration. In this scenario, chemoattractants stimulate the binding of WDR26 to Gβγ to promote Gβγ-mediated signal transduction for chemotaxis. The increased Gβγ signaling may in turn result in the recruitment of RACK1 to bind

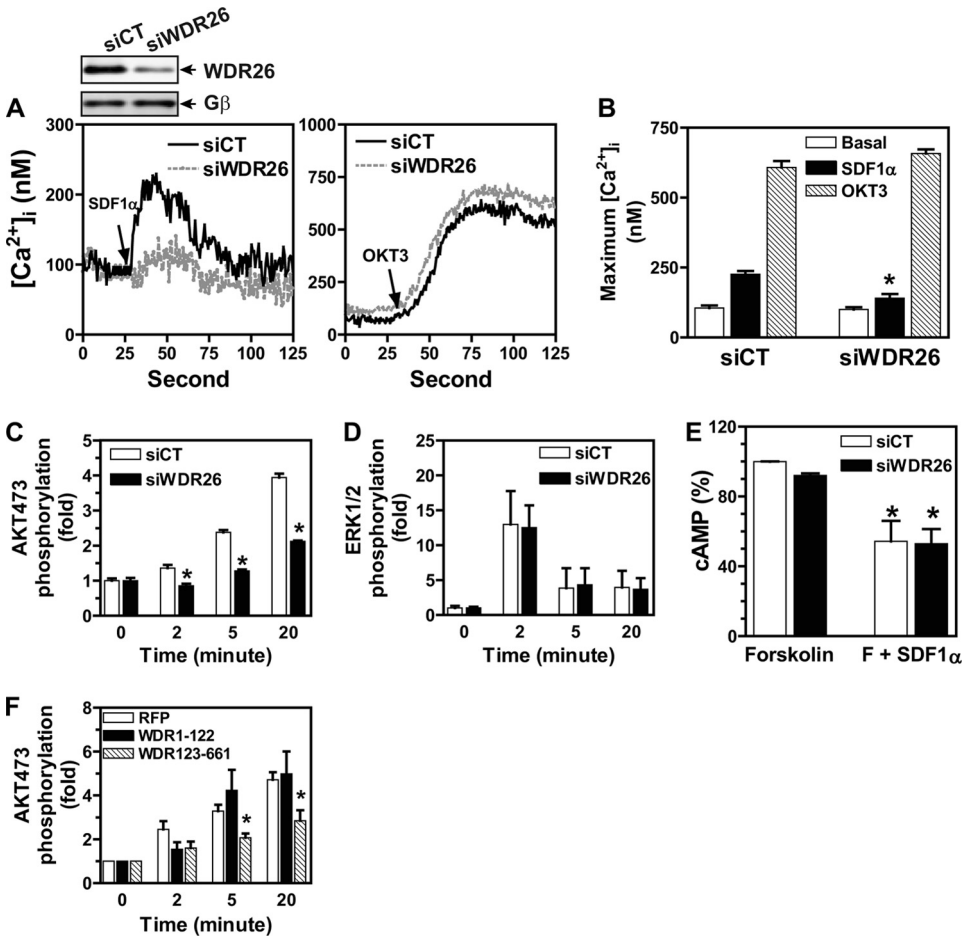

FIGURE 7. **WDR26 is required for Gβγ-mediated signal transduction.** Jurkat T cells were transiently transfected with a control (*siCT*) or WDR26 siRNA (*siWDR26*). *A* and *B*, Ca^{2+} signaling. Cells were loaded with Fura2-AM and stimulated with SDF1α (50 nM) or OKT3 (5 μg/ml). The change in intracellular Ca^{2+} concentration ($[Ca^{2+}]_i$) was monitored at 340/380 nm. Representative data are shown in *A*. Maximum $[Ca^{2+}]_i$ calculated from more than five separate experiments is shown in *B*. *, $p < 0.05$ indicates significance *versus* siCT. *C* and *D*, AKT (*C*) and ERK1/2 (*D*) phosphorylation stimulated by SDF1α (50 nM). Data are expressed as fold-increase over unstimulated control after the levels of phosphorylated proteins are normalized with that of total proteins. *, $p < 0.05$ indicates significance *versus* siCT ($n = 3–5$). *E*, cAMP production. cAMP was measured in the transfected Jurkat T cells treated with or without SDF1α (50 nM) in the presence of forskolin (10 μM) for 20 min. Data are expressed as percentage of forskolin-stimulated cAMP production in siCT-transfected Jurkat T cells. *, $p < 0.05$ indicates significance *versus* forskolin ($n = 4$). *F*, SDF1α-stimulated AKT phosphorylation in Jurkat T cells transfected with the indicated constructs. *, $p < 0.05$ indicates significance *versus* RFP ($n = 3–4$).

Gβγ, which possibly functions in a negative feedback loop to decrease or terminate Gβγ-mediated signal transduction. Further studies to uncover the molecular basis for the regulation of WDR26 and RACK1 interaction with Gβγ will be important for revealing the mechanisms by which WDR26 and RACK1 are involved in the precise regulation of Gβγ signaling for leukocyte migration.

WDR26 was recently identified as one of several WD40 proteins associated with the CUL4-DDB 1 ubiquitin E3 ligase complex (35). These WD40 proteins have been proposed to act as adaptors that direct the CUL4-DDB1 ubiquitin ligase to specific substrates, thereby regulating ubiquitin-dependent proteolysis (55, 56). It is conceivable that WDR26 may regulate PI3Kγ and PLCβ activation by controlling the expression level of a critical regulator through CUL4-DDB1 ubiquitin ligase. However, our data indicate that this is unlikely because inhibition of WDR26 does not affect the expression level of numerous proteins we examined, ranging from the receptor to effectors and regulators. Moreover, silencing CUL4 could not recapitulate the inhibitory effect of WDR26 suppression on Jurkat T cell chemotaxis, suggesting that the activity of CUL4 is not involved in leukocyte chemotaxis.

WDR26 contains a conserved WD40 repeat domain that is present in a large family of proteins confined primarily to eukaryotic organisms (25, 26). The WD40 domain in these proteins has no intrinsic enzymatic activity but often functions as an adaptor/scaffold to orchestrate protein-protein interactions for the regulation of the specificity, efficacy, and localization of multiple signaling pathways. Given that the WD40 domain of WDR26 is involved in binding Gβγ, it will be interesting to determine in future studies whether WDR26 utilizes the WD40 domain as a scaffold to form a macroprotein complex with Gβγ and its effectors, thereby promoting Gβγ-mediated signal transduction.

Our data demonstrate that WDR26 plays a critical role in regulating Gβγ signaling and leukocyte migration. In addition to regulating leukocyte function, Gβγ controls a variety of physiological processes, including heart rate and neuronal excitability (4). Excessive Gβγ signaling has been implicated in diverse pathological conditions, such as heart failure (57, 58), inflammation (59), and tumor cell growth/metastasis (36, 60,

61). Given that WDR26 is ubiquitously expressed (33), future studies will be important to determine whether WDR26 contributes to the regulation of Gβγ signaling in other normal cellular processes and if its dysregulation contributes to aberrant Gβγ signaling and disease.

Acknowledgment—We greatly appreciated Caitlin Runne for critical reading of the manuscript.

REFERENCES

1. Oldham, W. M., and Hamm, H. E. (2008) *Nat. Rev. Mol. Cell Biol.* **9,** 60–71
2. Tesmer, J. J. (2010) *Nat. Struct. Mol. Biol.* **17,** 650–652
3. Rickert, P., Weiner, O. D., Wang, F., Bourne, H. R., and Servant, G. (2000) *Trends Cell Biol.* **10,** 466–473
4. Smrcka, A. V. (2008) *Cell Mol. Life Sci.* **65,** 2191–2214
5. Janetopoulos, C., and Firtel, R. A. (2008) *FEBS Lett.* **582,** 2075–2085
6. Neptune, E. R., and Bourne, H. R. (1997) *Proc. Natl. Acad. Sci. U.S.A.* **94,** 14489–14494
7. Arai, H., Tsou, C. L., and Charo, I. F. (1997) *Proc. Natl. Acad. Sci. U.S.A.* **94,** 14495–14499
8. Tan, W., Martin, D., and Gutkind, J. S. (2006) *J. Biol. Chem.* **281,** 39542–39549
9. Peracino, B., Borleis, J., Jin, T., Westphal, M., Schwartz, J. M., Wu, L., Bracco, E., Gerisch, G., Devreotes, P., and Bozzaro, S. (1998) *J. Cell Biol.* **141,** 1529–1537
10. Sotsios, Y., Whittaker, G. C., Westwick, J., and Ward, S. G. (1999) *J. Immunol.* **163,** 5954–5963
11. Hirsch, E., Katanaev, V. L., Garlanda, C., Azzolino, O., Pirola, L., Silengo, L., Sozzani, S., Mantovani, A., Altruda, F., and Wymann, M. P. (2000) *Science* **287,** 1049–1053
12. Li, Z., Dong, X., Dong, X., Wang, Z., Liu, W., Deng, N., Ding, Y., Tang, L., Hla, T., Zeng, R., Li, L., and Wu, D. (2005) *Nat. Cell Biol.* **7,** 399–404
13. Sasaki, T., Irie-Sasaki, J., Jones, R. G., Oliveira-dos-Santos, A. J., Stanford, W. L., Bolon, B., Wakeham, A., Itie, A., Bouchard, D., Kozieradzki, I., Joza, N., Mak, T. W., Ohashi, P. S., Suzuki, A., and Penninger, J. M. (2000) *Science* **287,** 1040–1046
14. Servant, G., Weiner, O. D., Herzmark, P., Balla, T., Sedat, J. W., and Bourne, H. R. (2000) *Science* **287,** 1037–1040
15. Liu, L., Puri, K. D., Penninger, J. M., and Kubes, P. (2007) *Blood* **110,** 1191–1198
16. Bach, T. L., Chen, Q. M., Kerr, W. T., Wang, Y., Lian, L., Choi, J. K., Wu, D., Kazanietz, M. G., Koretzky, G. A., Zigmond, S., and Abrams, C. S. (2007) *J. Immunol.* **179,** 2223–2227
17. Dong, X., Mo, Z., Bokoch, G., Guo, C., Li, Z., and Wu, D. (2005) *Curr. Biol.* **15,** 1874–1879
18. Kunisaki, Y., Nishikimi, A., Tanaka, Y., Takii, R., Noda, M., Inayoshi, A., Watanabe, K., Sanematsu, F., Sasazuki, T., Sasaki, T., and Fukui, Y. (2006) *J. Cell Biol.* **174,** 647–652
19. Kunisaki, Y., Tanaka, Y., Sanui, T., Inayoshi, A., Noda, M., Nakayama, T., Harada, M., Taniguchi, M., Sasazuki, T., and Fukui, Y. (2006) *J. Immunol.* **176,** 4640–4645
20. Li, Z., Hannigan, M., Mo, Z., Liu, B., Lu, W., Wu, Y., Smrcka, A. V., Wu, G., Li, L., Liu, M., Huang, C. K., and Wu, D. (2003) *Cell* **114,** 215–227
21. Srinivasan, S., Wang, F., Glavas, S., Ott, A., Hofmann, F., Aktories, K., Kalman, D., and Bourne, H. R. (2003) *J. Cell Biol.* **160,** 375–385
22. Welch, H. C., Coadwell, W. J., Ellson, C. D., Ferguson, G. J., Andrews, S. R., Erdjument-Bromage, H., Tempst, P., Hawkins, P. T., and Stephens, L. R. (2002) *Cell* **108,** 809–821
23. Swaney, K. F., Huang, C. H., and Devreotes, P. N. (2010) *Annu. Rev. Biophys.* **39,** 265–289
24. Chen, S., Spiegelberg, B. D., Lin, F., Dell, E. J., and Hamm, H. E. (2004) *J. Mol. Cell Cardiol.* **37,** 399–406
25. Stirnimann, C. U., Petsalaki, E., Russell, R. B., and Müller, C. W. (2010) *Trends Biochem. Sci.* **35,** 565–574
26. Smith, T. F. (2008) *Subcell. Biochem.* **48,** 20–30
27. Smith, T. F., Gaitatzes, C., Saxena, K., and Neer, E. J. (1999) *Trends Biochem. Sci.* **24,** 181–185
28. Dell, E. J., Connor, J., Chen, S., Stebbins, E. G., Skiba, N. P., Mochly-Rosen, D., and Hamm, H. E. (2002) *J. Biol. Chem.* **277,** 49888–49895
29. Chen, S., Dell, E. J., Lin, F., Sai, J., and Hamm, H. E. (2004) *J. Biol. Chem.* **279,** 17861–17868
30. Chen, S., Lin, F., and Hamm, H. E. (2005) *J. Biol. Chem.* **280,** 33445–33452
31. Chen, S., Lin, F., Shin, M. E., Wang, F., Shen, L., and Hamm, H. E. (2008) *Mol. Biol. Cell* **19,** 3909–3922
32. Zhao, J., Liu, Y., Wei, X., Yuan, C., Yuan, X., and Xiao, X. (2009) *Neurosci. Lett.* **460,** 66–71
33. Zhu, Y., Wang, Y., Xia, C., Li, D., Li, Y., Zeng, W., Yuan, W., Liu, H., Zhu, C., Wu, X., and Liu, M. (2004) *J. Cell. Biochem.* **93,** 579–587
34. Wei, X., Song, L., Jiang, L., Wang, G., Luo, X., Zhang, B., and Xiao, X. (2010) *Biochem. Biophys. Res. Commun.* **393,** 860–863
35. Higa, L. A., Wu, M., Ye, T., Kobayashi, R., Sun, H., and Zhang, H. (2006) *Nat. Cell Biol.* **8,** 1277–1283
36. Tang, X., Sun, Z., Runne, C., Madsen, J., Domann, F., Henry, M., Lin, F., and Chen, S. (2011) *J. Biol. Chem.* **286,** 13244–13254
37. Ford, C. E., Skiba, N. P., Bae, H., Daaka, Y., Reuveny, E., Shekter, L. R., Rosal, R., Weng, G., Yang, C. S., Iyengar, R., Miller, R. J., Jan, L. Y., Lefkowitz, R. J., and Hamm, H. E. (1998) *Science* **280,** 1271–1274
38. Preininger, A. M., Van Eps, N., Yu, N. J., Medkova, M., Hubbell, W. L., and Hamm, H. E. (2003) *Biochemistry* **42,** 7931–7941
39. Phillips, W. J., Wong, S. C., and Cerione, R. A. (1992) *J. Biol. Chem.* **267,** 17040–17046
40. Phillips, W. J., and Cerione, R. A. (1992) *J. Biol. Chem.* **267,** 17032–17039
41. Takesono, A., Horai, R., Mandai, M., Dombroski, D., and Schwartzberg, P. L. (2004) *Curr. Biol.* **14,** 917–922
42. Hannigan, M., Zhan, L., Li, Z., Ai, Y., Wu, D., and Huang, C. K. (2002) *Proc. Natl. Acad. Sci. U.S.A.* **99,** 3603–3608
43. Allen, W. E., Zicha, D., Ridley, A. J., and Jones, G. E. (1998) *J. Cell Biol.* **141,** 1147–1157
44. Takeda, K., Sasaki, A. T., Ha, H., Seung, H. A., and Firtel, R. A. (2007) *J. Biol. Chem.* **282,** 11874–11884
45. Kollet, O., Spiegel, A., Peled, A., Petit, I., Byk, T., Hershkoviz, R., Guetta, E., Barkai, G., Nagler, A., and Lapidot, T. (2001) *Blood* **97,** 3283–3291
46. Peled, A., Petit, I., Kollet, O., Magid, M., Ponomaryov, T., Byk, T., Nagler, A., Ben-Hur, H., Many, A., Shultz, L., Lider, O., Alon, R., Zipori, D., and Lapidot, T. (1999) *Science* **283,** 845–848
47. Grynkiewicz, G., Poenie, M., and Tsien, R. Y. (1985) *J. Biol. Chem.* **260,** 3440–3450
48. Xu, J., Wang, F., Van Keymeulen, A., Herzmark, P., Straight, A., Kelly, K., Takuwa, Y., Sugimoto, N., Mitchison, T., and Bourne, H. R. (2003) *Cell* **114,** 201–214
49. Wang, F. (2009) *Cold Spring Harbor Perspect. Biol.* **1,** a002980
50. Cathcart, M. K. (2009) *J. Lipid Res.* **50,** (suppl.) S231–236
51. Chen, L., Iijima, M., Tang, M., Landree, M. A., Huang, Y. E., Xiong, Y., Iglesias, P. A., and Devreotes, P. N. (2007) *Dev. Cell* **12,** 603–614
52. Mishra, R. S., Carnevale, K. A., and Cathcart, M. K. (2008) *J. Exp. Med.* **205,** 347–359
53. Cara, D. C., Kaur, J., Forster, M., McCafferty, D. M., and Kubes, P. (2001) *J. Immunol.* **167,** 6552–6558
54. Heit, B., Robbins, S. M., Downey, C. M., Guan, Z., Colarusso, P., Miller, B. J., Jirik, F. R., and Kubes, P. (2008) *Nat. Immunol.* **9,** 743–752
55. Jackson, S., and Xiong, Y. (2009) *Trends Biochem. Sci.* **34,** 562–570
56. Biedermann, S., and Hellmann, H. (2011) *Trends Plant Sci.* **16,** 38–46
57. Casey, L. M., Pistner, A. R., Belmonte, S. L., Migdalovich, D., Stolpnik, O., Nwakanma, F. E., Vorobiof, G., Dunaevsky, O., Matavel, A., Lopes, C. M., Smrcka, A. V., and Blaxall, B. C. (2010) *Circ. Res.* **107,** 532–539
58. Harding, V. B., Jones, L. R., Lefkowitz, R. J., Koch, W. J., and Rockman, H. A. (2001) *Proc. Natl. Acad. Sci. U.S.A.* **98,** 5809–5814
59. Lehmann, D. M., Seneviratne, A. M., and Smrcka, A. V. (2008) *Mol. Pharmacol.* **73,** 410–418
60. Bookout, A. L., Finney, A. E., Guo, R., Peppel, K., Koch, W. J., and Daaka, Y. (2003) *J. Biol. Chem.* **278,** 37569–37573
61. Kirui, J. K., Xie, Y., Wolff, D. W., Jiang, H., Abel, P. W., and Tu, Y. (2010) *J. Pharmacol. Exp. Ther.* **333,** 393–403